JACS
JOURNAL OF THE AMERICAN CHEMICAL SOCIETY
Communication
pubs.acs.org/JACS

Stepwise Ligand Exchange for the Preparation of a Family of Mesoporous MOFs

Tao Li,[†] Mark T. Kozlowski,[†] Evan A. Doud,[†] Maike N. Blakely,[‡] and Nathaniel L. Rosi*[,†]

[†]Department of Chemistry, University of Pittsburgh, Pittsburgh, Pennsylvania 15260, United States
[‡]Department of Chemistry, Chatham University, Pittsburgh, Pennsylvania 15232, United States

Supporting Information

ABSTRACT: A stepwise ligand exchange strategy is utilized to prepare a series of isoreticular **bio-MOF-100** analogues. Specifically, *in situ* ligand exchange with progressively longer dicarboxylate linkers is performed on single crystalline starting materials to synthesize products with progressively larger mesoporous cavities. The new members of this series of materials, **bio-MOFs 101−103**, each exhibit permanent mesoporosity and pore sizes ranging from ∼2.1−2.9 nm and surface areas ranging from 2704 to 4410 m^2/g. The pore volume for **bio-MOF 101** is 2.83 cc/g. **Bio-MOF-102** and **103** have pore volumes of 4.36 and 4.13 cc/g, respectively. Collectively, these data establish this unique family of MOFs as one of the most porous reported to date.

The realization of mesoporosity in metal−organic frameworks (MOFs) has opened the door to new potential applications for this class of periodic porous materials.[1] Several mesoporous MOFs have been reported.[1c] However, the overwhelming majority has a distribution of micropores (<2 nm) and mesopores (2−50 nm); micropores can gate entry to the mesopores and therefore limit the size of species that are allowed to freely diffuse and migrate throughout the structure. Only a few mesoporous MOFs exhibit continuous uninterupted mesoporous channels.[2] Cubic **Bio-MOF-100**[2a] has continuous and interconnected mesoporous channels running throughout its structure. It is one of only two reported MOF materials having a pore volume exceeding 4 cc/g,[2a,3] and we have shown that it can be used as a scaffold for organizing large molecules, including short peptides.[4]

In this communication, we report three new isoreticular analogues of **bio-MOF-100**: **bio-MOF-101**, **102**, and **103**. We utilize a stepwise ligand exchange strategy to prepare these materials in which shorter ligands are replaced by longer ligands in what appears to be a crystal to crystal transformation. **Bio-MOF-102** and **bio-MOF-103** each have pore volumes that exceed 4 cc/g; together with **bio-MOF-100**, they represent three of only four reported MOFs that exceed this threshold.[3] To our knowledge, this report documents the first demonstration that ligand exchange can be utilized to systematically increase the pore dimensions of MOF materials.[5] This strategy is very promising because (1) it represents a potentially universal method for increasing MOF porosity; (2) the nature of the ligand exchange process avoids the possibility of interpenetration, provided that a noninterpenetrated MOF is used as the starting material; and (3) it allows access to products that may be thermodynamically unfavorable.

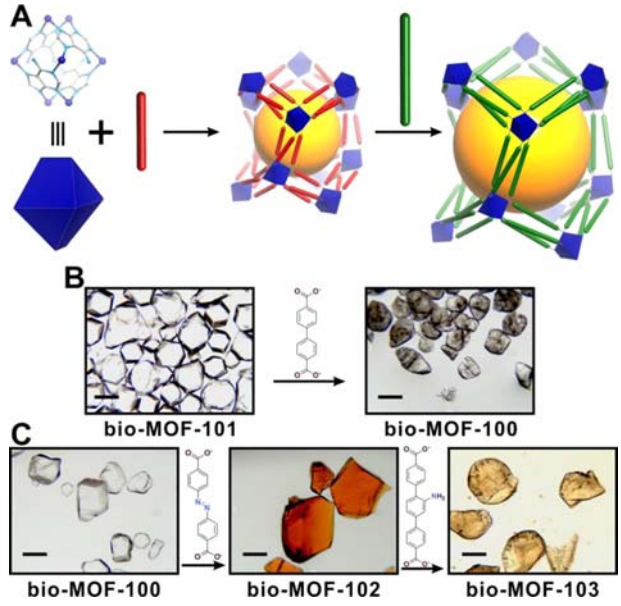

Figure 1. Scheme depicting pore expansion strategy (A). As-synthesized **bio-MOF-101** was converted to **bio-MOF-100** via ligand exchange with BPDC (B). BPDC in **bio-MOF-100** was replaced with ABDC to yield **bio-MOF-102**; thereafter ABDC in **bio-MOF-102** was replaced with NH_2-TPDC to yield **bio-MOF-103** (C). Light microscope images of the crystalline MOFs have scale bars representing 0.2 mm.

We began this study by first attempting to synthesize isoreticular analogues of **bio-MOF-100** using various linear dicarboxylate linkers. **Bio-MOF-100** adopts the highly open ***lcs*** net[6] and consists of zinc-adeninate clusters ($Zn_8Ad_4O_2^{8+}$; Ad = adeninate) periodically linked with 4,4′-biphenyldicarboxylate (BPDC).[2a] Although we succeeded in preparing **bio-MOF-101**, the isoreticular analogue of **bio-MOF-100** having 2,6-naphthalenedicarboxylate (NDC) linkers, at this stage we were unable to prepare analogues with linkers longer than BPDC. This prompted us to explore ligand exchange as a strategy for accessing more porous analogues of **bio-MOF-100**.

To realize this design strategy, we first studied the conversion between **bio-MOF-101** and **bio-MOF-100** (Figure 1A,B). **Bio-**

Received: April 16, 2013
Published: May 20, 2013

   dx.doi.org/10.1021/ja403810k | *J. Am. Chem. Soc.* 2013, 135, 11688−11691

MOF-101 was thoroughly washed with *N*,*N*′-dimethylformamide (DMF) and subsequently soaked in a 0.05 M H_2-BPDC/DMF/NMP (DMF:NMP = 1:1 ; NMP = *N*-methylpyrolidinone) solution for 24 h in a 75 °C oven; the solution was removed, replaced with a fresh H_2-BPDC solution, and the mixture was again heated at 75 °C for 24 h.

Upon inspection using an optical microscope, the product crystals were mostly transparent and slightly cracked (Figure 1B). ^{1}H NMR spectra of the dissolved crystalline product revealed only the presence of adenine and BPDC linkers; no NDC was detected, indicating that it was completely replaced by BPDC (Figure S1).

Having successfully converted **bio-MOF-101** to **bio-MOF-100** through ligand exchange, we endeavored to expand the pores of **bio-MOF-100** by using a similar process to replace BPDC with the slightly longer azobenzene-4,4′-dicarboxylate (ABDC) and the much longer 2′-amino-1,1′:4,1″-terphenyl-4,4″-dicarboxylate (NH_2-TPDC). Due to their characteristic dark orange (ABDC) and light orange color (NH_2-TPDC), we expected to observe a crystal color change after successful ligand exchange. When soaked in an H_2-ABDC solution, the colorless **bio-MOF-100** crystals did indeed transform into dark orange crystals without noticeable cracks (Figure 1C). We monitored this process by imaging a single crystal of **bio-MOF-100** at different time points during reaction (Figure S10). It is clear from these images that the crystal remains intact and progresses from colorless to pale orange to dark orange throughout the course of the ligand exchange reaction. The resulting new crystalline material, named **bio-MOF-102**, was then soaked in an H_2-NH_2-TPDC solution to yield light orange crystals, named **bio-MOF-103** (Figure 1C). ^{1}H NMR spectra of dissolved samples of **bio-MOF-102** revealed the presence of adenine and ABDC and a trace amount of residual BPDC (Figure S2). Complete ligand exchange was not observed for the entirety of the product crystals in the transformation of **bio-MOF-102** to **bio-MOF-103**: integration of appropriate peaks in the ^{1}H NMR spectrum of the dissolved products indicate ∼85% NH_2-TPDC and ∼15% residual ABDC (Figure S3).

After characterizing the chemical composition following the ligand exchange reactions, we studied the structures of the product crystals. We loaded single crystals of each product onto an X-ray diffractometer and collected diffraction data for unit cell analysis. The unit cell parameters (Table 1) of a product crystal from the reaction of **bio-MOF-101** with BPDC closely matched the reported values,[2a] indicating successful conversion of **bio-MOF-101** to **bio-MOF-100**. A product crystal of the **bio-MOF-100**/ABDC exchange reaction had a cubic unit cell with $a = b = c = 75.24$ Å, which is ∼6 Å longer than the unit cell parameter of **bio-MOF-100**. We were able to collect and solve a complete data set for the single crystal, which verified that it was indeed an isoreticular analogue of **bio-MOF-100** and that BPDC was completely replaced by ABDC. Finally, a product crystal of the **bio-MOF-102**/NH_2-TPDC exchange reaction had a cubic unit cell with $a = b = c = 82.254$ Å, which is ∼7 Å longer than that observed for **bio-MOF-102**. However, these crystals were extremely weakly diffracting, so at this stage we resorted to constructing a model of the **bio-MOF-103** structure using the single crystal unit cell parameters (Table S3).

Table 1. Unit Cell Parameters Obtained from Single Crystal X-ray Experiments

unit cell parameters	$a = b = c =$ (Å)	literature value of a (Å)	$\alpha = \beta = \gamma =$ (deg)
Bio-MOF-101	62.04	N/A	90
Bio-MOF-100	68.90	69.12[2a]	90
Bio-MOF-102	75.24	N/A	90
Bio-MOF-103	82.25	N/A	90

Powder X-ray diffraction (PXRD) patterns were collected to examine the phase purity of the bulk product (Figure 2). These data confirm that (1) **bio-MOF-100** was produced from **bio-MOF-101** (Figure 2A); (2) **bio-MOF-102** was produced from **bio-MOF-100** (Figure 2B); and (3) **bio-MOF-103** was produced from **bio-MOF-102** (Figure 2C). In all cases, the principal diffraction lines shifted toward lower angles after longer linkers replaced shorter linkers. The product MOF powder patterns are in very good agreement with those simulated from single-crystal diffraction data or from the structural model, in the case of **bio-MOF-103**. In each case, no reactant diffraction lines were observed in the product MOF, even for **bio-MOF-103** in which complete ligand exchange was not observed. Since three linkers connect neighboring $Zn_8Ad_4O_2^{8+}$ building blocks together within the structure, the longest linker should determine the distance between two building blocks. These data support the conclusion that ligand exchange reactions result in complete structural transformation for the entire sample.

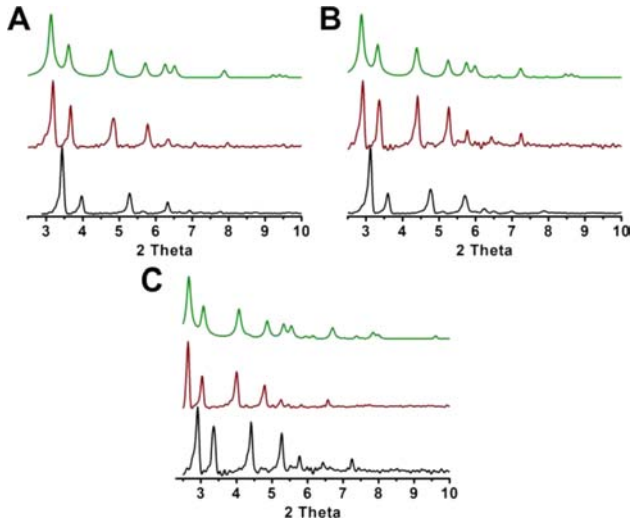

Figure 2. (A) PXRD patterns of as-synthesized **bio-MOF-101** (black), **bio-MOF-100** obtained from ligand exchange (red) and **bio-MOF-100** simulated from crystal structure (green); (B) PXRD patterns of as-synthesized **bio-MOF-100** (black), **bio-MOF-102** (red) and **bio-MOF-102** simulated from single crystal data (green); (C) PXRD patterns of **bio-MOF-102** (black), **bio-MOF-103** (red) and **bio-MOF-103** simulated from single crystal model (green).

We expected to observe a volume change for the solid materials after replacing short linkers with long linkers. A certain amount of **bio-MOF-101** crystals was loaded into an NMR tube (1.2 cm of tube length, Figure 3A). Stepwise ligand exchange reactions were performed within the NMR tube (Supporting Information). After ligand exchange by BPDC and allowing the product to settle completely, the height of the sample increased to 1.5 cm. The **bio-MOF-100** product (Figure 3B) was reacted with H_2-ABDC to yield orange **bio-MOF-102** (Figure 3C), which has an expanded sample height of 2.3 cm. Finally, the **bio-MOF-102** product (Figure 3C) was

dx.doi.org/10.1021/ja403810k | J. Am. Chem. Soc. 2013, 135, 11688−11691

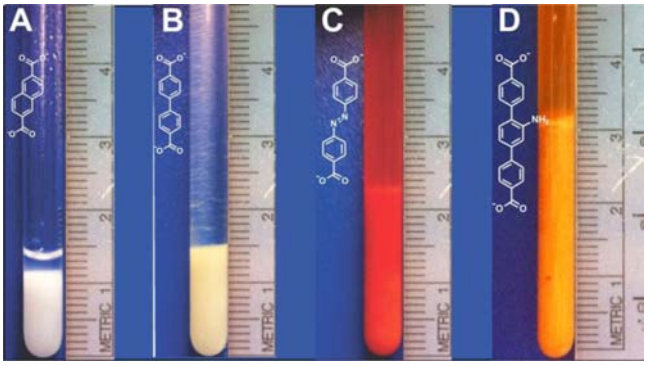

Figure 3. Volume expansion experiment showing as-synthesized **bio-MOF-101** (A), **bio-MOF-100** (B), **bio-MOF-102** (C), and **bio-MOF-103** (D).

reacted with H_2-NH_2-TPDC. The light orange product crystals of **bio-MOF-103** (Figure 3D) have a height of ∼3.2 cm. This continuous change in sample height offers qualitative visual proof of the volume change of the crystals after ligand exchange.

The porosities of **bio-MOF-101** and the products of ligand exchange, **bio-MOF-100**, **102**, and **103**, were investigated by N_2 gas adsorption at 77 K. Crystalline samples were completely exchanged with ethanol and activated using established methods.[8] Each material exhibits a Type IV adsorption isotherm characteristic of mesoporous materials (Figure 4A). The analogue with the shortest linker, **bio-MOF-101**, adsorbs the least amount of N_2 and has a calculated pore volume of 2.83 cc/g. The **bio-MOF-100** sample prepared herein adsorbed 2444 cc/g N_2 which is slightly lower than the previously reported value.[2a] We surmise that this may be due to defects

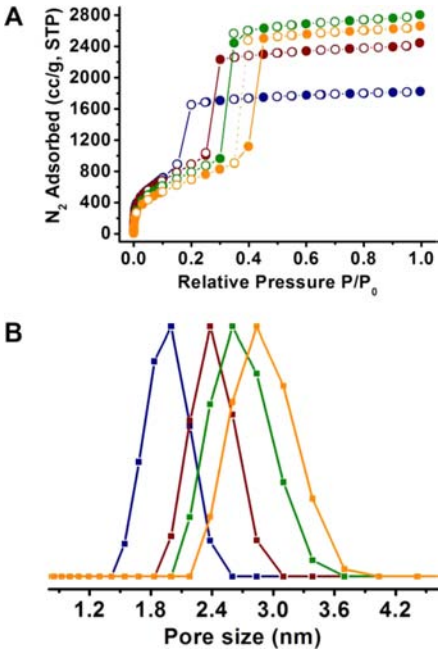

Figure 4. (A) N_2 adsorption isotherms of **bio-MOF-101** (navy), **bio-MOF-100** (red), **bio-MOF-102** (green), **bio-MOF-103** (orange) at 77 K. (B) normalized pore size distribution (PSD) of **bio-MOF-101** (navy), **bio-MOF-100** (red), **bio-MOF-102** (green), **bio-MOF-103** (orange) calculated by quenched solid state functional theory (QSDFT) method.[7]

created during the ligand exchange process. As expected, **bio-MOF-102** and **103** show the highest N_2 uptakes and exhibit calculated pore volumes of 4.36 and 4.13 cc/g, respectively. The pore volume of **bio-MOF-102** exceeded the reported pore volume of **bio-MOF-100**, making it the second most porous MOF reported in terms of the pore volume metric.[3] We note that only the isotherm for **bio-MOF-103** shows hysteresis upon desorption; we hypothesize that this may be due to the incomplete exchange of ABDC by NH_2-TPDC (*vide supra*). We calculated the pore size distribution for each material using the QSDFT method (Figure 4B).[7] These data definitively demonstrate that the ligand exchange method can be used to systematically increase the pore size of this class of mesoporous bio-MOFs from ∼2.00 to 2.84 nm, which agrees well with the pore sizes predicted from the crystal structures (2.1 to 2.9 nm).

In summary, we have demonstrated that using ligand exchange, a short linker molecule in a MOF can be replaced with a longer one to produce a more porous isoreticular analogue without sacrificing loss of crystallinity. This process can be applied sequentially to yield product MOFs with increasingly larger pore sizes. We predict that this method can also be used to isolate new MOFs that cannot be prepared using traditional synthetic methods. We have established herein that, collectively, **bio-MOFs 100−103** are one of the most porous families of MOF materials based on the important metric of total pore volume.

■ ASSOCIATED CONTENT

Ⓢ Supporting Information

Additional synthetic procedures, instrumentations, X-ray experiments, ^{1}H NMR. This material is available free of charge via the Internet at http://pubs.acs.org.

■ AUTHOR INFORMATION

Corresponding Author

nrosi@pitt.edu

Notes

The authors declare no competing financial interest.

■ ACKNOWLEDGMENTS

A portion of this work was performed under the RES contract DE-FE0004000 as part of the National Energy Technology Laboratory's Regional University Alliance (NETL-RUA), a collaborative initiative of the NETL. The authors also thank the Petersen Institute for Nanoscience and Engineering (PINSE) for access to XRPD instrumentation and the Mechanical Engineering and Materials Science (MEMS) Department for access to SEM instrumentation.

■ REFERENCES

(1) (a) Wang, X.-S.; Ma, S.; Sun, D.; Parkin, S.; Zhou, H.-C. *J. Am. Chem. Soc.* **2006**, *128*, 16474. (b) Fang, Q.-R.; Makal, T.; Young, M.; Zhou, H.-C. *Comments Inorg. Chem.* **2010**, *31*, 165. (c) Xuan, W.; Zhu, C.; Liu, Y.; Cui, Y. *Chem. Soc. Rev.* **2012**, *41*, 1677.

(2) (a) An, J.; Farha, O. K.; Hupp, J. T.; Pohl, E.; Yeh, J. I.; Rosi, N. L. *Nat. Commun.* **2012**, *3*, 604. (b) Morris, W.; Volosskiy, B.; Demir, S.; Gandara, F.; McGrier, P. L.; Furukawa, H.; Cascio, D.; Stoddart, J. F.; Yaghi, O. M. *Inorg. Chem.* **2012**, *51*, 6443. (c) Feng, D.; Gu, Z. Y.; Li, J. R.; Jiang, H. L.; Wei, Z.; Zhou, H. C. *Angew. Chem., Int. Ed.* **2012**, *51*, 10307. (d) Chen, Y.; Hoang, T.; Ma, S. *Inorg. Chem.* **2012**, *51*, 12600. (e) Deng, H.; Grunder, S.; Cordova, K. E.; Valente, C.; Furukawa, H.; Hmadeh, M.; Gandara, F.; Whalley, A. C.; Liu, Z.;

Asahina, S.; Kazumori, H.; O'Keeffe, M.; Terasaki, O.; Stoddart, J. F.; Yaghi, O. M. *Science* **2012**, *336*, 1018.
(3) Farha, O. K.; Eryazici, I.; Jeong, N. C.; Hauser, B. G.; Wilmer, C. E.; Sarjeant, A. A.; Snurr, R. Q.; Nguyen, S. T.; Yazaydin, A. O.; Hupp, J. T. *J. Am. Chem. Soc.* **2012**, *134*, 15016.
(4) Liu, C.; Li, T.; Rosi, N. L. *J. Am. Chem. Soc.* **2012**, *134*, 18886.
(5) (a) Kondo, M.; Furukawa, S.; Hirai, K.; Kitagawa, S. *Angew. Chem., Int. Ed.* **2010**, *49*, 5327. (b) Park, H. J.; Cheon, Y. E.; Suh, M. P. *Chem.—Eur. J.* **2010**, *16*, 11662. (c) Li, J.-R.; Zhou, H.-C. *Nat. Chem.* **2010**, *2*, 893. (d) Burnett, B. J.; Barron, P. M.; Hu, C.; Choe, W. *J. Am. Chem. Soc.* **2011**, *133*, 9984. (e) Burnett, B. J.; Choe, W. *Dalton Trans.* **2012**, *41*, 3889. (f) Kim, M.; Cahill, J. F.; Fei, H.; Prather, K. A.; Cohen, S. M. *J. Am. Chem. Soc.* **2012**, *134*, 18082. (g) Cohen, S. M. *Chem. Rev.* **2012**, *112*, 970. (h) Park, J.; Wang, Z. U.; Sun, L. B.; Chen, Y. P.; Zhou, H. C. *J. Am. Chem. Soc.* **2012**, *134*, 20110. (i) Kim, M.; Cahill, J. F.; Su, Y.; Prather, K. A.; Cohen, S. M. *Chem. Sci.* **2012**, *3*, 126. (j) Karagiaridi, O.; Bury, W.; Sarjeant, A. A.; Stern, C. L.; Farha, O. K.; Hupp, J. T. *Chem. Sci.* **2012**, *3*, 3256.
(6) Delgado Friedrichs, O.; O'Keeffe, M.; Yaghi, O. M. *Acta Crystallogr., Sect. A* **2003**, *59*, 515.
(7) Ravikovitch, P. I.; Neimark, A. V. *Langmuir* **2006**, *22*, 11171.
(8) Nelson, A. P.; Farha, O. K.; Mulfort, K. L.; Hupp, J. T. *J. Am. Chem. Soc.* **2008**, *131*, 458.